ASSIMILATION OF MODIS OBSERVATIONS OF SNOWPACK SURFACE PROPERTIES INTO ONE YEAR OF SPATIALIZED ENSEMBLE SNOWPACK SIMULATIONS AT A FIELD SITE IN THE FRENCH ALPS

Bertrand Cluzet[1,*], Jesus Revuelto[1], Matthieu Lafaysse[1], Marie Dumont[1], Emmanuel Cosme[2], François Tuzet[1]

[1] *Univ. Grenoble Alpes, Université de Toulouse, Météo-France, CNRS, Centre d'Études de la Neige, Grenoble, France*
[2] *UGA-CNRS-IRD, IGE, Grenoble, France*

ABSTRACT: Detailed snowpack modelling is crucial for avalanche hazard forecasting, glaciological modelling and hydrological studies, but its use is currently limited by its level of uncertainty. Ensemble forecasting approaches are commonly used to quantify the associated uncertainties. Combined with satellite data assimilation, they can help reduce the modelling errors. In this study, an ensemble simulation chain accounting for both meteorological and modelling uncertainties was used to simulate snowpack conditions in the mountain range ("massif") of Grandes-Rousses covering an area of about 500km^2 for various elevations, aspects and slopes during the 2013-2014 winter. This modelling chain involves perturbed meteorological forcings from ARPEGE-SAFRAN analysis system and multi-physics ensemble version of snowpack model Crocus called Ensemble System Crocus (ESCROC). In addition, visible and near infrared satellite data from MODIS sensor were retrieved in the same area and study period. Such data convey precious information on the snowpack surface impurities content, snow microstructure properties and snowpack extent. A comparison with ensemble outputs is presented to assess their potential for data assimilation with a particle filter. Results show that there is a high potential of assimilation of MODIS observations into ensemble semi-distributed simulations of snowpack if transformed variables are used to tackle observation systematic biases. This could lead to a significant improvement in snowpack modelling accuracy at the massif scale in a near future.

Keywords: snow modelling, ensemble, remote sensing, MODIS, data assimilation, particle filter

1. INTRODUCTION

Multilayer physically-based models such as SNOWPACK (Lehning et al., 2002) and Crocus (Vionnet et al., 2012) are commonly used to monitor and forecast snowpack properties at a local scale or within a mountain range. They require meteorological forcings able to account for the specificities of complex mountainous terrain. In France, the operational modelling system is based on SAFRAN meteorological analyses (Durand et al., 1993) over relatively homogeneous areas of about 1000 km^2 (so-called *massifs*) which only assimilates surface meteorological observations. They are used to force Crocus snowpack model at the same scale and for various aspects and slopes. However, snowpack simulations from these modelling chains suffer for numerous error sources, including meteorological forcing and snowpack model errors (Raleigh et al., 2015), and unresolved spatial variability. This can drastically limit the interest of the model chain for many operational applications and scientific studies and it has to be tackled.

At the same time, in-situ observations of snowpack properties are sparse and with limited spatial representativity. In this context, high-resolution observations (250m) of snowpack visible and near infrared reflectances from MODIS satellite sensor provide precious information about the snowpack extent and surface properties such as light absorbing impurities content (LAIC) and snow grain optical size (Specific Surface Area, SSA) (Dozier et al., 2009). Retrieval algorithms such as MODImLab have been developped and constantly improved to adapt it to mountainous complex topographies (Sirguey, 2009). This product has been proven to outperform MODIS MOD10 product in many studies (Dumont et al. (2012), Charrois et al. (2013)) and is used here. LAIC and SSA are the main variables controlling radiative transfer in snow in the visible and near-infrared spectrum (Libois et al., 2013). Recent developments in snowpack model Crocus (TARTES radiative transfer scheme (Libois et al., 2015), LAIC modelling (Tuzet et al., 2017),

*Corresponding author address:
Bertrand Cluzet
Météo-France-CNRS, CNRM UMR 3589
Centre d'Études de la Neige
1441 Rue de la Piscine
38400 Saint-Martin-d'Hères, France;
tel: +33476633764
email: bertrand.cluzet@meteo.fr

and impact of snow metamorphism on SSA (Carmagnola et al., 2013)) make it possible to link these properties with the surface reflectance. This allows straightforward comparison between observed and simulated reflectances in MODIS spectral bands. Our goal is to assess the possibility of assimilating such products into spatialized snowpack simulations.
In the recent years, snowpack ensemble approaches emerged associated with the twofold aim of quantifying the uncertainties (Essery (2015), Lafaysse et al. (2017)) and using it in a data assimilation system (Charrois et al. (2016), Magnusson et al. (2017), Piazzi et al. (2018), Larue et al. (2018)). In these four studies, a Particle Filter with Sequential Importance Resampling (PF-SIR) was successfully used to improve snowpack ensemble simulations accuracy at the local scale. Here, we explore the potential of extending such a system to spatialized simulations and through the combination of a meteorological ensemble and a multiphysical system.
Thus, our main goal is to compare spatialized ensemble snowpack simulations with remotely-sensed observations of snow reflectance, and assess whether such observations could be assimilated using a PF-SIR.

2. DATA & METHODS

2.1. Model

ESCROC (Lafaysse et al., 2017) is the multiphysical ensemble version of Crocus handling 7774 different model configurations. In this study 35 members were randomly drawn between each observation dates among the 1944 ESCROC members using TARTES radiative transfer scheme and combined with the explicit scheme for the evolution of the snowpack impurities content of Tuzet et al. (2017). This ensemble was forced by 35 perturbed SAFRAN meterological forcings generated with perturbations described in Charrois et al. (2016). MOCAGE chemistry-transport model (Josse et al., 2004) black carbon (BC) and Dust wet and dry deposition fluxes were added to the meteorological forcings and perturbed using an order 1 multiplicative Auto-Regressive process with a decorrelation time of 3 hours and random perturbations following $\mathcal{N}(\mu = 0, \sigma^2 = 0.24)$, in a similar approach as for the meteorological variables. Simulations on 187 topographical classes ranging from 600 to 3600 masl by 300m elevation bands, 0, 20 and 40 degrees of slope and 8 aspects (so-called ”semi-distributed” geometry) were carried out in the Grandes-Rousses massif (French Alps), during the 2013-2014 winter.

2.2. Snow observations

MODIS top of atmosphere reflectance in the first seven spectral bands are available at 250 to 500m spatial resolution depending on the channel. We extracted and post-processed these data in a 15x16km region (3060 pixels) including part of the Grandes-Rousses geographical extent and centered on Col du Lautaret field site during 2013-2014 winter with MODImLab retrieval algorithm. MODImLab accounts for atmospherical radiative transfer, direct and diffuse contribution, multiple topographical reflection, terrain shading and snow reflectance anisotropy. Reflectance in visible bands (1,3,4) is mostly affected by the impurities content in snow (such as black carbon and mineral dust) whereas in the near infrared spectral bands (2,5,6,7) it depends mostly on the grain size and snow metamorphism (Dozier et al., 2009). The resulting products have a 250m resolution in all seven bands. 17 acquisition dates with good geometrical acquisition properties (sensor zenithal angle $\leq 30°$), and clear sky were selected. Pixels with forest, clouds, shadows, and Snow Cover Fraction (SCF) ≤ 0.85, were filtered out consistently with Mary et al. (2013).
The remaining pixels were classified according to the topographical classes of our modelling system. As a result, most of the 187 classes handle over a tenth of so-called ”distributed observations” for most dates. Classes where the mean SCF was under 0.85 were not considered. Finally, for each snow-covered class, the mean reflectances were computed, producing so-called ”semi-distributed observations”.
Dumont et al. (2012) consider that the error magnitude associated with MODImLab-retrieved broadband albedo is about $\pm 10\%$ of the value, which is consistent with the observational error standard deviations of 0.053 and 0.10 for band 3 and 5 respectively prescribed in Charrois et al. (2016), though this assessment is a challenging task (Sirguey, 2009).

2.3. Feasability of data assimilation with the PF-SIR

To assess the potential of applying the PF-SIR in our spatialized ensemble simulation, a thorough comparison of observed and openloop (i.e. whithout assimilation) simulated reflectances is necessary. Firstly, time variations of the ensemble and the observations should be consistent with the expected evolution of top LAIC and SSA along the season. Secondly, it is expected that the observation often lies within the ensemble, i.e. that the ensemble spread is larger than the difference between the ensemble median and the observation (innovation), and than the observation error. Innovations must also not be systematically biased. Otherwise it is

likely for the PF-SIR to collapse (Charrois et al., 2016). Thirdly, Pearson correlations (R) between the ensemble median and semi-distributed observations timeseries will give additional information on the potential of information and the feasability of data assimilation (provided that second condition can be satisfied). If timeseries are badly correlated, this means that it is likely that observations carry substantial information valuable for the ensemble, but that data assimilation of such different datasets will be a challenge (Reichle et al., 2004). The opposite (R close to 1) will imply that there should be less valuable information for the model within observations, but that the similarity between datasets should make data assimilation more likely to function.
In order to address discrepancies between the two datasets that would make straightforward data assimilation impossible, our strategy is if possible to avoid using any bias correction, data-driven techniques, or any kind of class-dependant matching between model and observations that would hide or compensate for systematic model errors. The three conditions will be assessed in Sec.3.1. Solutions to improve compliance to those conditions will be investigated in Sec.3.2.

3. RESULTS

3.1. Comparison of observed and simulated variables

As a first step, comparisons between openloop ensemble and observations were carried out in the classes where the observation process is the most reliable, i.e. with low probability of being mixed/rocky (20° maximal slope) and with large enough pixel populations over the whole snow season (1800-3000 masl). Figs. 1a and 1b show timeseries of ensemble and observations in MODIS bands 3 and 5 in a sun facing slope at 2400m. Fig.1a shows consistent time variations between semi-distributed observations and the ensemble in those topographical classes. Decrease in reflectance in both bands from November to beginning of December and on January 12th is consistent with extended periods without snowfall, leading to BC deposition on top of the snowpack and coarsening of the top layer grains. Then, all dates until end of February correspond to recent snowfalls, with low impurities content and high SSA, hence high reflectance values in both bands. Finally, the end of the snow season causes melted forms with low SSA (i.e. low band 5 reflectance) to form at the surface while two Saharan dust deposition events (end of February, end of March) cause drops in band 3 reflectance. All those events clearly appear in both ensemble and observation timeseries.
However, there is a notably strong bias in band 3, together with an apparent under dispersion of the ensemble in this band (compared with Sec. 2.3 observation errors) during most of the winter.
In the infra-red band 5 (Fig.1b), the agreement is notably better, with a lower bias and a higher spread, closer to typical errors and observed variability. Both Figs. 1a and 1b seem to indicate a statistical relationship between the observations and the ensemble.

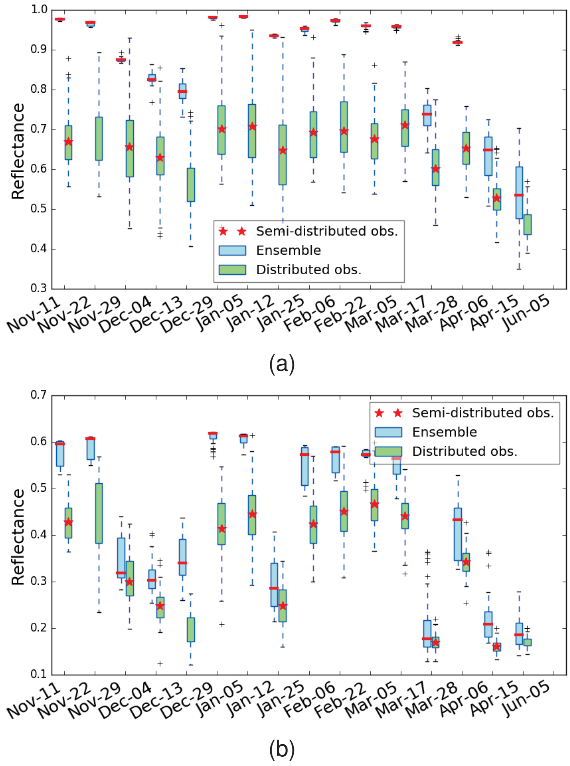

Figure 1: Boxplot timeseries of the openloop ensemble (blue), distributed observations (green) and semi-distributed observations (stars) at (2400m, SE, 20°) class in MODIS band 3 (1a) and band 5 (1b) for the 17 observation dates. Red lines denote medians of the ensemble.

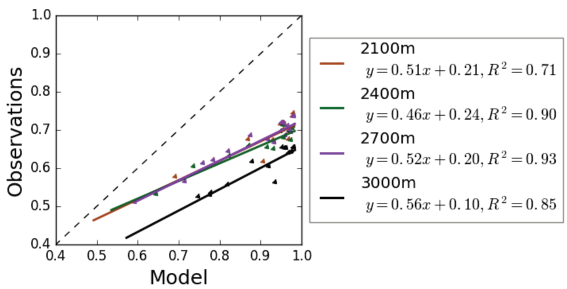

Figure 2: Regressions of semi-distributed observations and ensemble median in MODIS band 3, at four different elevations, SE aspect, 20° slope.

Assuming a time-invariant relationship, regressions were carried out between the timeseries of the ensemble median and the semi-distributed observations inside each topographical class. As an example, Fig.2 shows a linear relationship between the ensemble median and the semi-distributed observations in band 3, at four different elevation classes, with R^2 values over 0.7.

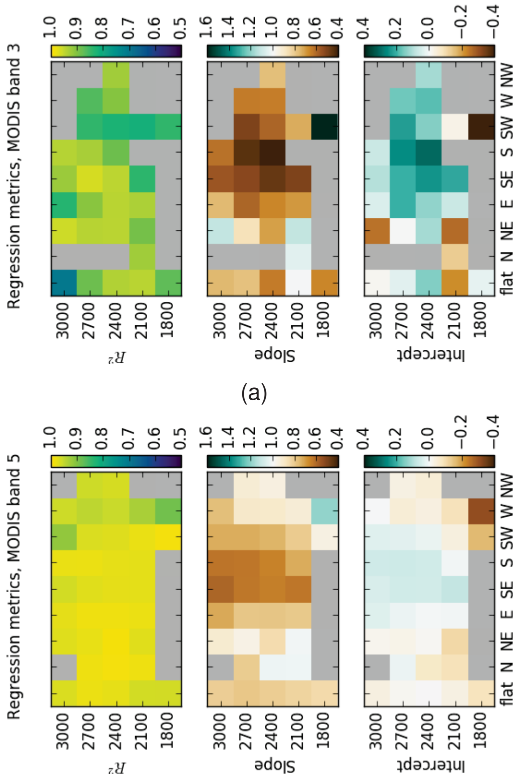

(a)

(b)

Figure 3: Regression statistics between ensemble median and semi-distributed observations for all aspects at 20° slope and flat, for five elevation classes in MODIS band 3 (3a) and 5 (3b). Only regressions with p-values under 0.01 are displayed.

To assess a potential topographical dependency of this relationship, statistics of linear regressions between observations and ensemble are shown in Figs. 3a and 3b in all the considered classes. Both figures show overall significant and high correlations between the ensemble median and the observations, R^2 being higher in the sun facing slopes (flat, SE, S, and E), and higher in band 5 than in band 3. Slope is always under 1, consistently with Fig. 2. In addition regression parameters seem to depend more on aspect than on elevation.
To summarize, time variations of the ensemble and observations are physically consistent, and comparison of the openloop ensemble versus the observations is promising since it reveals a strong linear agreement in this semi-distributed geometry. However, data assimilation with a particle filter is not possible in this situation due to the strong diagnosed biases and the apparent mismatch between the spread of the ensemble and the observation errors. Finally, high significant R values were exhibited for both bands. Following Sec.3.2 shows ways to improve the fulfilment of Sec.2.3 conditions.

3.2. Spectral bands reflectance ratio

Computing a ratio between the reflectances in two different bands (so-called "band ratio") might reduce the discrepancy between observations and model. If successful, consistently with Sec.2.3, this correction would be much more satisfactory than for example, using regression coefficients from Figs. 3a and 3b to adjust the observations before assimilation.
To that aim, the ratio between bands 5 and 3 was computed. Fig.4 shows the temporal evolution of this variable. There is obviously a better match than for the raw reflectance values both in terms of mean values and spread. In many cases, the semi-distributed observation falls within the ensemble. Statistics of linear regression in Fig.5 show high R^2 values generally above 0.8, though it is slightly lower than for band 5. More interestingly, regression parameters are now centred around identity (Slope=1, Intercept=0) which clearly illustrates the better agreement (no systematic bias) of observations and model for this variable.

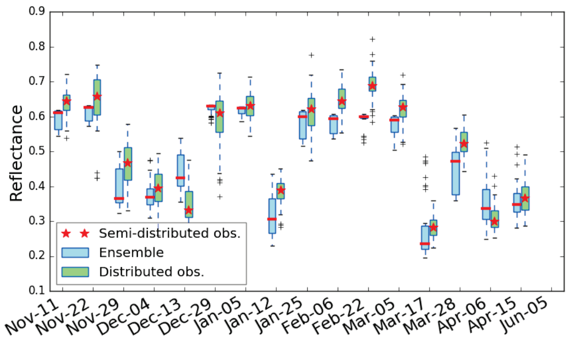

Figure 4: Same as for Fig. 1, for band ratio 5/3.

Rank diagrams are a powerful tool to assess the potential of ensemble assimilation algorithms (Piazzi et al., 2018). It consists in a frequency histogram of the rank of the observation within the ensemble. In our case of markedly under-dispersive ensemble, all the useful information content can be condensed to whether the rank is "under", "inside" or "over" the ensemble. Tab.1 provides this condensed rank histogram aggregated over all dates and topographical classes between 1800 and 3000 masl for the three variables. It depicts a high bias of the ensemble regarding semi-distributed observations in both bands 3 and 5, the observation being under the ensemble for 71 to 93% of the occurencies and only 7 to 29% inside. Nevertheless, the rank dia-

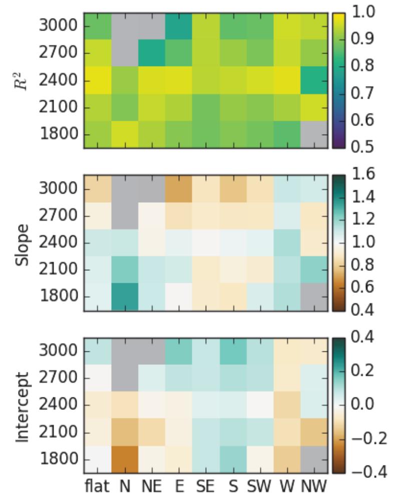

Figure 5: Same as Figs. 3a and 3b, for band ratio 5/3.

gram for band ratio is highly improved with respect to bands 3 and 5 separately, the observation being in the ensemble 59% of the time. Though the ensemble remains slightly under-dispersive, this last result is really encouraging for data assimilation.

variable	under (%)	inside (%)	over (%)
band 3	93	7	0
band 5	71	29	0
ratio 5/3	8	59	33

Table 1: Summary of rank diagrams aggregated over all dates and considered classes (453 occurencies).

4. DISCUSSION

4.1. *Sources of observation errors*

Though it is clear that the ensemble reflectance can be biased, observed values in the visible part of the spectrum are obviously unrealistically low, with 0.8 reflectance for fresh snow in band 1 on December 29^{th} for instance. This low bias of MODImLab retrieved observations could be consistent with a misestimation of the atmospheric absorption and scattering in MODImLab algorithm over the Alps as pointed out in (Davaze et al., 2018).

4.2. *Limitations of the openloop ensemble*

As pointed out in Fig.1a, the ensemble seems to be highly underdispersive during the core winter, making it adventurous to assimilate any observation with a PF-SIR during those dates. There are several possible explanations coming from the ensemble simulation itself : underdispersion of LAIC for band 3, SSA for band 5, and of meteorological forcings for both bands. First, a comparison with observed impurities content at Col du Lautaret field site during 2016-2017 and 2017-2018 winters will help assessing the performance of the ensemble in representing impurities concentrations and uncertainties, evaluate the uncertainties coming from MOCAGE impurities deposition fluxes and calibrate the perturbations.Such a low dispersion, however, could just be an evidence that the information content of observations in band 3 is lower at those altitudes during the core winter, when frequent snowfall occurs, burying higher BC/Dust concentrated layers (light penetration in this band is only of a few cm). Nonetheless, this spectral band still provides valuable information during dry periods, after dust deposition events and when surface melting brings layers with high LAIC up to the surface.

Despite model band 5 is underdispersive to a lesser extent, ensemble performance can be improved in this band too. Indeed, MODIS band 5 is only affected by snow SSA of the top first millimeters (Carmagnola et al., 2013). SSA generally decreases with snow metamorphism, from high values up to 80 m^2/kg for fresh snow to around 5 m^2/kg for melt forms. Though ESCROC multiphysics includes different metamorphism laws (Carmagnola et al. (2014) and Flanner and Zender (2006)), falling snow SSA is prescribed to 65 m^2/kg, though this value can vary a lot with the type of precipitation particles (Carmagnola et al., 2014). An improvement could be (at least) to perturb this value. In addition, our simulation account for the effects of wind transport and wind-induced metamorphism. These processes have a significant effects on surface snow properties and could be accounted for including Crocus-SYTRON blowing snow scheme (Vionnet et al., 2018) to the multiphysics configurations of ESCROC. Lastly, Tuzet et al. (2017) showed that LAIC can substantially influence band 5 reflectance through indirect impact of the radiative budget on snow grain metamorphism.

Finally, underdispersion of both bands may also be explained by a lack of dispersion in the meteorological forcings (impurities apart) causing too similar snow surface properties between the members. Statistical perturbations of meteorological forcings as used in this study rely on calibrations based on in-situ measurements. This may deteriorate the physical consistency between meteorological variables, generate some biases (Piazzi et al., 2018) and may be insufficient to describe the temporal and spatial variability of the uncertainty. Future work will investigate the potential of ensemble of meteorological models such as PEARP, which may offer a more consistent way to force our simulations (Vernay et al., 2015).

5. CONCLUSION & FUTURE WORK

This study showed a first assessment of the potential of the assimilation of remotely-sensed snowpack reflectance in a spatialized modelling environment close to an operational one. Though an obvious bias in all bands has been showed, the time variation of the ensemble and the observation are highly correlated. Comparison with field measurements at Col du Lautaret will be carried out in the near future and help confirm our hypothesis that this bias is mostly observational. Future developments will include a more physical assessment of meteorological uncertainties with the use of PEARP-SAFRAN as a meteorological forcing and assessment of the quality of MOCAGE impurities forcings. Developments in ESCROC ensemble to better account for the properties of the freshly fallen snow could be a lead as well.
In addition some leads were investigated on how to deal with reflectance biases for assimilation by computing a reflectance ratio between spectral bands. the significantly improved agreement between observations and ensemble simulations gives us a good confidence on the potential for operational data assimilation of such data in Meteo-France's operational snowpack modelling chain in the near future. It is a first step from point-scale assimilation to operational semi-distibuted and large-scale consistent data assimilation in snowpack models.

REFERENCES

Carmagnola, C. M., Domine, F., Dumont, M., Wright, P., Strellis, B., Bergin, M., Dibb, J., Picard, G., Libois, Q., Arnaud, L., and Morin, S. (2013). Snow spectral albedo at summit, greenland: measurements and numerical simulations based on physical and chemical properties of the snowpack. *The Cryosphere*, 7(4):1139–1160.

Carmagnola, C. M., Morin, S., Lafaysse, M., Domine, F., Lesaffre, B., Lejeune, Y., Picard, G., and Arnaud, L. (2014). Implementation and evaluation of prognostic representations of the optical diameter of snow in the surfex/isba-crocus detailed snowpack model. *The Cryosphere*, 8(2):417–437.

Charrois, L., Cosme, E., Dumont, M., Lafaysse, M., Morin, S., Libois, Q., and Picard, G. (2016). On the assimilation of optical reflectances and snow depth observations into a detailed snowpack model. *The Cryosphere*, 10(3):1021–1038.

Charrois, L., Dumont, M., Sirguey, P., Morin, S., Lafaysse, M., and Karbou, F. (2013). Comparing different modis snow products with distributed simulation of the snowpack in the french alps. In *Proceedings of the International Snow Science Workshop*, Innsbruck, Austria.

Davaze, L., Rabatel, A., Arnaud, Y., Sirguey, P., Six, D., Letreguilly, A., and Dumont, M. (2018). Monitoring glacier albedo as a proxy to derive summer and annual surface mass balances from optical remote-sensing data. *The Cryosphere*, 12(1):271–286.

Dozier, J., Green, R. O., Nolin, A. W., and Painter, T. H. (2009). Interpretation of snow properties from imaging spectrometry. *Remote Sensing of Environment*, 113:S25–S37.

Dumont, M., Gardelle, J., Sirguey, P., Guillot, A., Six, D., and Arnaud, A. R. Y. (2012). Linking glacier annual mass balance and glacier albedo retrieved from modis data. *The Cryosphere*, 6:1527–1539.

Durand, Y., Brun, E., Mérindol, L., Guyomarc'h, G., Lesaffre, B., and Martin, E. (1993). A meteorological estimation of relevant parameters for snow models. *Ann. Glaciol.*, 18:65–71.

Essery, R. (2015). A factorial snowpack model (fsm 1.0). *Geosci. Model Dev.*, 8:3867–3876.

Flanner, M. G. and Zender, C. S. (2006). Linking snowpack microphysics and albedo evolution. *J. Geophys. Res.*, 111:D12208.

Josse, B., Simon, P., and Peuch, V.-H. (2004). Radon global simulations with the multiscale chemistry and transport model mocage. *Tellus B: Chemical and Physical Meteorology*, 56(4):339–356.

Lafaysse, M., Cluzet, B., Dumont, M., Lejeune, Y., Vionnet, V., and Morin, S. (2017). A multiphysical ensemble system of numerical snow modelling. *The Cryosphere*, 11(3):1173.

Larue, F., Royer, A., De Sève, D., Roy, A., Picard, G., Vionnet, V., and Cosme, E. (2018). Simulation and assimilation of passive microwave data using a snowpack model coupled to a calibrated radiative transfer model over north-eastern canada. *Water Resources Research*.

Lehning, M., Bartelt, P., Brown, B., Fierz, C., and Satyawali, P. (2002). A physical SNOWPACK model for the Swiss avalanche warning. part II: snow microstructure. *Cold Reg. Sci. Technol.*, 35(3):147 – 167.

Libois, Q., Picard, G., Arnaud, L., Dumont, M., Lafaysse, M., Morin, S., and Lefebvre, E. (2015). Summertime evolution of snow specific surface area close to the surface on the Antarctic Plateau. *The Cryosphere*, 9(6):2383–2398.

Libois, Q., Picard, G., France, J., Arnaud, L., Dumont, M., Carmagnola, C. M., and King, M. (2013). Influence of grain shape on light penetration in snow. *The Cryosphere*, 7:1803–1818.

Magnusson, J., Winstral, A., Stordal, A. S., Essery, R., and Jonas, T. (2017). Improving physically based snow simulations by assimilating snow depths using the particle filter. *Water Resources Research*, 53(2):1125–1143.

Mary, A., Dumont, M., Dedieu, J.-P., Durand, Y., Sirguey, P., Milhem, H., Mestre, O., Negi, H. S., Kokhanovsky, A. A., Lafaysse, M., and Morin, S. (2013). Intercomparison of retrieval algorithms for the specific surface area of snow from near-infrared satellite data in mountainous terrain, and comparison with the output of a semi-distributed snowpack model. *The Cryosphere*, 7:741–761.

Piazzi, G., Thirel, G., Campo, L., and Gabellani, S. (2018). A particle filter scheme for multivariate data assimilation into a point-scale snowpack model in alpine environment. *The Cryosphere Discussions*.

Raleigh, M. S., Lundquist, J. D., and Clark, M. P. (2015). Exploring the impact of forcing error characteristics on physically based snow simulations within a global sensitivity analysis framework. *Hydrol. Earth Syst. Sci.*, 19(7):3153–3179.

Reichle, R. H., Koster, R. D., Dong, J., and Berg, A. A. (2004). Global soil moisture from satellite observations, land surface models, and ground data: Implications for data assimilation. *Journal of Hydrometeorology*, 5(3):430–442.

Sirguey, P. (2009). Simple correction of multiple reflection effects in rugged terrain. *Int. J. Remote Sens.*, 30:1075–1081.

Tuzet, F., Dumont, M., Lafaysse, M., Picard, G., Laurent, A., Voisin, D., Lejeune, Y., Charrois, L., Nabat, P., and Morin, S. (2017). A multilayer physically based snowpack model simulating direct and indirect radiative impacts of light-absorbing impurities in snow. *The Cryosphere*, 11(6):2633.

Vernay, M., Lafaysse, M., Merindol, L., Giraud, G., and Morin, S. (2015). Ensemble forecasting of snowpack conditions and avalanche hazard. *Cold. Reg. Sci. Technol.*, 120:251–262.

Vionnet, V., Brun, E., Morin, S., Boone, A., Martin, E., Faroux, S., Le-Moigne, P., and Willemet, J.-M. (2012). The detailed snowpack scheme Crocus and its implementation in SURFEX v7.2. *Geosci. Model. Dev.*, 5:773–791.

Vionnet, V., Guyomarc'h, G., Lafaysse, M., Naaim-Bouvet, F., Giraud, G., and Deliot, Y. (2018). Operational implementation and evaluation of a blowing snow scheme for avalanche hazard forecasting. *Cold Regions Science and Technology*, 147:1–10.